

Electrons and phonons at sub-Kelvin temperatures: validation of the disorder-mediated scattering theory

I. J. Maasilta, J. T. Karvonen, J. M. Kivioja*, and L. J. Taskinen

NanoScience Center, Department of Physics, P.O. Box 35, FIN-40014 University of Jyväskylä, Finland

(Dated: October 4, 2003)

We have used symmetric normal metal-insulator-superconductor (NIS) tunnel junction pairs, known as SINIS structures, for ultrasensitive thermometry in the temperature range 50 - 700 mK. By Joule heating the electron gas and measuring both the electron and the lattice temperatures simultaneously, we show for the first time that the electron-phonon (e-p) scattering rate in a well studied and common disordered thin-film material (Cu) follows a T^4 temperature dependence. This power law is indicative e-p coupling mediated by vibrating disorder, in contrast to the previously observed T^3 and T^2 laws.

Although the interaction between conduction electrons and thermal phonons is elementary for many processes and phenomena at low temperatures, there are still relatively few experimental studies that conclusively support the theoretical description, particularly for typical disordered thin film samples. Several earlier results [1, 2, 3] indicated that even for disordered films, the temperature dependence for the electron-phonon (e-p) scattering rate $1/\tau_{e-p}$ follows the power law expected for pure samples with coupling to longitudinal phonons only: $1/\tau_{e-p} \sim T^3$ [4]. These results confirmed the relation $P = \Sigma\Omega(T_e^5 - T_p^5)$ between heating power P and electron and phonon temperatures T_e and T_p in a volume Ω , and it is widely used for thin film metallic samples at low temperatures (Σ is a material dependent parameter). However, the theory for disordered thin films [5, 6, 7, 8] predicts that the scattering rate from vibrating disorder (impurities, boundaries) is $1/\tau_{e-p} \sim T^4$ in the limit $ql < 1$, where q is the wavevector of the dominant thermal phonons and l the electron mean free path. This leads to the relation

$$P = \Sigma'\Omega(T_e^6 - T_p^6), \quad (1)$$

a result that has not been widely confirmed. In fact, we are not aware of any observation of it in standard normal metal films like Cu, Al, Au etc., and only suggestive evidence exists for strongly disordered ($l \sim 1$ nm) Ti, Hf [9] and Bi [10] films.

Here, we report the first observation of disorder-mediated electron-phonon (e-p) scattering in ordinary, evaporated Cu thin films. We have measured the rate at which electrons in a normal metal (Cu) wire overheat, when DC power is applied to it by Joule heating. This technique has been shown [1, 2, 3] to give the energy-loss rate directly, in contrast to the temperature dependence of the weak localization resistance [11], which gives the dephasing rate [12]. The overheating rate is determined directly by measuring the electron temperature with the help of symmetric normal metal-insulator-superconductor (NIS) tunnel junction pairs, known as SINIS structures. SINIS-thermometers have been shown

[13, 14, 15] to be extremely sensitive thermometers, operating at the lowest experimentally achievable temperatures. Therefore, they are also candidates for ultrasensitive microbolometers [16, 17] in the sub-Kelvin temperature range.

Samples used in this work have two Cu normal metal wires of length ~ 500 μm , and width 300 nm, separated by a distance 2 μm and electrically isolated from each other, as shown in the SEM image [Fig. 1(a)]. They were fabricated by e-beam lithography and three-angle shadow-mask evaporation technique on thermally oxidized (oxide thickness 250 nm) Si substrates, with two film thicknesses $t = 45$ nm and 90 nm. The deposition was done by e-beam evaporation in a UHV chamber with a growth rate $\sim 2 - 3$ $\text{\AA}/\text{s}$. The normal metal wires were connected to the measurement circuit by superconducting Al leads. One pair of leads forms SINIS tunnel junctions for each wire, and are used to measure the electron temperature. These tunnel junctions were formed by thermal oxidation of the Al films in 50 mbar of O_2 for 5 min. In contrast, the junctions connecting the lower wire to a voltage source (Fig. 1) are NS-junctions without tunneling barriers, and are used to heat the sample. Clean NS-junctions have a small electrical resistance compared to the residual low-temperature resistance of the wire (250 and 700 Ω for the film thicknesses 90 and 45 nm, respectively). Thus, for low enough heating voltages the NS-junctions are biased within the superconducting gap Δ of the leads, and the process of Andreev reflection can take place making the junctions good thermal insulators despite being electrically conducting. When this takes place, we can achieve conditions in which the wire is uniformly Joule heated [18]. In addition, the thermal resistance of the tunnel junctions is estimated to be at least an order of magnitude larger than the thermal resistance due to the e-p coupling, R_{e-p} , at the temperature range of this experiment[20], and can be neglected in the analysis.

From the residual resistances and the dimensions of the wires we can estimate the electron mean free paths, yielding $l \approx 35$ nm for the samples with $t = 45$ nm, and $l \approx 50$ nm, for the samples with $t = 90$ nm. Since l

appears to be a significant fraction of the film thickness for both films, we surmise that boundary scattering is important in these samples. Using a transverse sound velocity $c_t = 2500$ m/s for Cu [21], we estimate that $ql = 2.82kT_p l/(\hbar c_t) \leq 1$ at phonon temperatures T_p below 195 mK and 135 mK for the thin and thick samples, respectively.

All measurements were performed by current biasing the two SINIS thermometers and measuring their DC voltages simultaneously [Fig 1(b)] in a dilution refrigerator with a base temperature ≈ 60 mK. The thermometers were calibrated by varying the bath temperature (T_{bath}) of the refrigerator very slowly, to ensure the sample stage was in equilibrium with the bath. The temperature of the sample stage was measured with a calibrated Ruthenium Oxide thermometer. Figure 2 shows an example of such a calibration measurement for both wires, including theoretical curves in addition to the experimental data. The theoretical curves (red) were calculated numerically from the BCS theory. This calculation has essentially no free parameters, since the current bias I is known and R_T , and Δ are determined independently from the I-V characteristics (not shown). The agreement with the data is good except at the very lowest temperatures, where a deviation can be seen in both junctions, more clearly so in the thermometer connected to the wire with extra NS-junctions. This deviation could arise by at least two major mechanisms: (i) a component of leakage current affects the measurement, and (ii) the electrons overheat at the low- T range (thermometer electron temperature T_e is higher than the sample stage temperature T_{bath}). We have ruled out (i) by directly measuring the responsivities dV/dP of the thermometers as a function of I using a lock-in amplifier (Fig. 2 inset). The theoretical dV/dP is a monotonically decreasing function of I . However, experimentally, at low I the responsivity deviates from theory and we find a maximum. Thus, by setting $I \geq 200$ pA into the BCS-theory regime problem (i) can be avoided. Moreover, the significant difference in the V vs T_{bath} data between the two thermometers clearly points to another source. Mechanism (ii), overheating by noise power P_{noise} , has been modeled with the help of the theory for e-p scattering and the Kapitza-resistance [22]:

$$P_{noise} = A(T_e^n - T_p^n) = B(T_p^4 - T_{bath}^4), \quad (2)$$

where $n = 4, 5, 6, A = \Sigma' \Omega$ and $B = \sigma S$ are parameters of the sample, S being the area of the Kapitza-boundary. Eliminating T_p from these equations, we get a relation $T_{bath} = [(T_e^n - P_{noise}/A)^{4/n} - P_{noise}/B]^{1/4}$, with two free parameters, P_{noise}/A and P_{noise}/B .

Including the heating model we obtain the result shown in Fig. 2 (blue) for the $t = 45$ nm sample, and a very similar result for the $t = 90$ nm sample (not shown).

Both calibration curves have essentially perfect fits to the model. Varying n did not have an effect on the goodness of the fit, so the calibration analysis does not bias our results and conclusions about the power of the e-p scattering. Moreover, the validity of our modeling is corroborated by the fact that the difference between the two wires is explained by a single scaling factor 30. This is expected, since A and B have the same values for both wires (equal sizes) so that only P_{noise} can vary. This variation is likely due to the NS-junctions: external noise sees a different impedance, determining how much noise power is dissipated in the sample.

Using the calibrated SINIS thermometers, we then studied what happened when only *one* of the wires is directly heated by Ohmic dissipation at $T_{bath} = 60$ mK. Heating power was applied by slowly ramping a DC voltage across the wire connected by the NS-junctions. The power P was determined by measuring the heating current and voltage across the wire directly in a 4-wire configuration. It should be noted that the SINIS circuit is fully floating with respect to the heating circuit, thus no heating current flows through the SIN junctions. In Fig 3 we plot the electron temperatures vs. P obtained from several sweeps for both wires for $t = 45$ nm sample (red) and for $t = 90$ nm sample (blue). As can be seen, *both* temperatures rise when heating power is increased. This means that the second wire is heated indirectly by phonons, since there is no direct electrical contact. Since these phonons can only strike the film from below, there must be a mechanism in the substrate to backscatter hot phonons generated in the first wire (corresponding to a distribution different from the thermal distribution at T_{bath}). Most likely, this scattering takes place in the oxide layer and/or at the interface between the oxide and the silicon substrate [23]. Also, bulk scattering of long wavelength phonons (the dominant thermal phonons at 100 mK have a wavelength of ~ 500 nm) in the crystalline Si lattice is negligible [24]. Clearly, above a few pW this phonon heating dominates the signal over the noise heating in the second wire (Fig 3). Thus, we can identify its temperature as the *phonon* temperature T_p , since all the power absorbed from the phonons has to be re-emitted back into the substrate (no net heat flow). Moreover, since the two wires are separated only by $\sim 2\mu\text{m}$, much longer than the lateral mean free path of phonons in SiO [22], the same T_p is seen by the first wire also. The conclusion is that we can simultaneously measure the electron and phonon temperatures of the first wire while it is being overheated. Boundary resistance between the Cu film and the substrate is not an issue, since the relevant phonon wavelengths are an order of magnitude longer than the Cu film thickness.

Looking back at Fig. 3, we see that when $P > P_{noise}$ both T_e and T_p initially scale as $(P/A)^{1/6}$ for both film thicknesses. Then in the thicker sample, a crossover to $(P/A)^{1/5}$ takes place at around $P = 100$ pW. Deviations

in the thinner sample also appear near $P = 1$ nW. These crossover points clearly correspond to the independently determined values of T_p , where $ql = 1$, as estimated earlier. Since $T_e^n \gg T_p^n$ for both $n = 5, 6$ in our experiment, we can say that the power laws obtained from Fig. 3 correspond to Eq. (1) when $ql < 1$, and indicate a transition to the common T^5 -law.

To obtain an alternative and more complete picture in the limit $ql < 1$ ($P < 75$ pW), Fig. 4 presents the data from the same runs for both samples in linear scale, with the power n in the expression $T_e^n - T_p^n$ varied from 4 to 6. It is very clear that $n = 4$ does not fit the data at all [Fig. 4(a)], showing that we are not dominated by the Kapitza resistance, or by e-p scattering mediated by static disorder [8]. Also, the expected theory for pure samples, $n = 5$ [Fig. 4(b)], clearly does not agree for either the thicker or the thinner sample in this limit, as the one-parameter linear fits through the origin do not fit the data well. (Two-parameter phenomenological linear fits show a reasonable result at the high power end, but are theoretically unjustified.) In contrast, $n = 6$ [Fig. 4(c)] gives consistent results, in agreement with Fig. 3. From the linear fits through the origin we get $\Sigma' = 1.4$ and $1.5 \times 10^{10} \text{ W/K}^6 \text{m}^3$ for the two film thicknesses. Comparing Σ' with the microscopic theory gives a reasonable result $c_t = 2300 \text{ m/s}$.

In conclusion, we have for the first time obtained clear evidence that the electron-phonon scattering rate scales with temperature as $1/\tau_{e-p} \sim T^4$ in disordered, evaporated Cu thin films. This power law corresponds to electrons scattering from transverse phonons mediated by boundaries, impurities, vacancies etc. that are vibrating together with the phonon mode. In contrast, e-p scattering in the presence of static disorder leads to $1/\tau_{e-p} \sim T^2$, a result that has been confirmed in many materials and samples [11]. Our result has several practical consequences. Compared to a lower power dependence, it is harder to cool the electrons with cold phonons, i.e. the electron gas decouples from the lattice more strongly at the lowest temperatures. Direct electron cooling [14, 15] then becomes more important. On the other hand, this means that a sensor based on hot electron effects is even more sensitive, since the ultimate noise equivalent power of such a detector is proportional to $1/R_{e-p}^{1/2}$. Similar results have recently been reported also for heavily doped, disordered silicon-on-insulator films [25]. We stress that in order to obtain $1/\tau_{e-p} \sim T^4$ the sample needs to have $ql < 1$, contain little non-vibrating disorder and have 3D phonons coupled to electrons by the deformation potential. We believe most earlier experiments do not satisfy all these three conditions (e.g. Ref. [1] has $ql > 1$, Ref. [26] has a suspended GaAs substrate, Refs. [2, 3, 27] studied alloys.)

We thank D.-V. Angel, M. P. Bruijn, A. N. Cleland, J. P. Pekola, A. Savin and A. Sergeev for discussions.

This work was supported by the Academy of Finland under the Finnish Center of Excellence Program 2000-2005 (Project No. 44875, Nuclear and Condensed Matter Physics Program at JYFL).

[*] Present Address: Low Temperature Laboratory, P. O. Box 2200, FIN-02015 HUT, Finland

- [1] M. L. Roukes, M. R. Freeman, R. S. Germain, R. C. Richardson, and M. B. Ketchen, Phys. Rev. Lett. **55**, 422 (1985).
- [2] M. Kanskar and M. N. Wybourne, Phys. Rev. Lett. **73**, 2123 (1994).
- [3] F. C. Wellstood, C. Urbina, and J. Clarke, Phys. Rev. B **49**, 5942 (1994).
- [4] V. F. Gantmakher, Rep. Prog. Phys. **37**, 317 (1974).
- [5] A. Schmid, Z. Phys. **259**, 421 (1973); in *Localization, Interaction and Transport Phenomena*, Springer 1985.
- [6] B. L. Altshuler, Zh. Eksp. Teor. Fiz. **75**, 1330 (1978) [Sov. Phys. JETP **48**, 670 (1986)].
- [7] M. Yu. Reizer and A. V. Sergeev, Zh. Eksp. Teor. Fiz. **90**, 1056 (1986) [Sov. Phys. JETP **63**, 616 (1986)].
- [8] A. Sergeev and V. Mitin, Phys. Rev. B **61**, 6041 (2000); Europhys. Lett. **51**, 641 (2000).
- [9] M. E. Gershenson, D. Dong, T. Sato, B. S. Karasik, and A. V. Sergeev, Appl. Phys. Lett. **79**, 2049 (2001).
- [10] Yu. F. Komnik, V. Yu. Kashirin, B. I. Belevtsev, and E. Yu. Beliaev, Phys. Rev. B **50**, 15 298 (1994).
- [11] For a recent review of the weak localization data, see J. J. Lin and J. P. Bird, J. Phys. Condens. Matter **14**, R501 (2002).
- [12] The dephasing rate can equal the energy loss rate if the electron-phonon interaction is the only dephasing mechanism present. In general, one can imagine many other dephasing channels that do not influence the energy loss rate, a prime example being the electron-electron interaction, which by definition cannot lower the energy of the electron gas as a whole.
- [13] J. M. Rowell and D. C. Tsui, Phys. Rev. B **14**, 2456 (1976).
- [14] M. Nahum, T. M. Eiles, and J. M. Martinis, Appl. Phys. Lett. **65**, 3123 (1994).
- [15] M. M. Leivo, J. P. Pekola, and D. V. Averin, Appl. Phys. Lett. **68**, 1996 (1996).
- [16] M. Nahum and J. Martinis, Appl. Phys. Lett. **63**, 3075 (1993).
- [17] L. Kuzmin, D. Chouvaev, M. Tarasov, P. Sundquist, M. Willander and T. Claeson, IEEE Trans. Appl. Supercond. **9**, 3186 (1999).
- [18] For much shorter but otherwise equivalent wires, the NS junctions are quickly biased above the gap, and the heat leak through them has to be taken into account in the analysis [19].
- [19] J. M. Kivioja, I. J. Maasilta, J. P. Pekola, and J. T. Karvonen, Physica E **18**, 21 (2003).
- [20] D. V. Anghel and J. P. Pekola, J. Low Temp. Phys. **123**, 197 (2001).
- [21] In the disordered limit, transverse phonon scattering is expected to be dominant over longitudinal phonons [8].
- [22] E. T. Swartz and R. O. Pohl, Rev. Mod. Phys. **61**, 605 (1989).

- [23] Since the contact area between the substrate and the sample stage is macroscopically large, the Kapitza resistance associated with it is small. We also attached the substrate to the sample stage by two different ways, with GE-7031 varnish and with silver paint, without any difference in results.
- [24] J. A. Shields, S. Tamura and J. P. Wolfe, Phys. Rev. B **43**, 4966 (1991).
- [25] P. Kivinen, A. Savin, M. Zgirski, P. Törmä, J. Pekola, M. Prunnila, and J. Ahopelto, J. Appl. Phys. **94**, 3201 (2003).
- [26] C. S. Yung, D. R. Schmidt, and A. N. Cleland, Appl. Phys. Lett. **81**, 31 (2002).
- [27] J. F. DiTusa, K. Lin, M. Park, M. S. Isaacson, and J. M. Parpia, Phys. Rev. Lett. **68**, 1156 (1992).

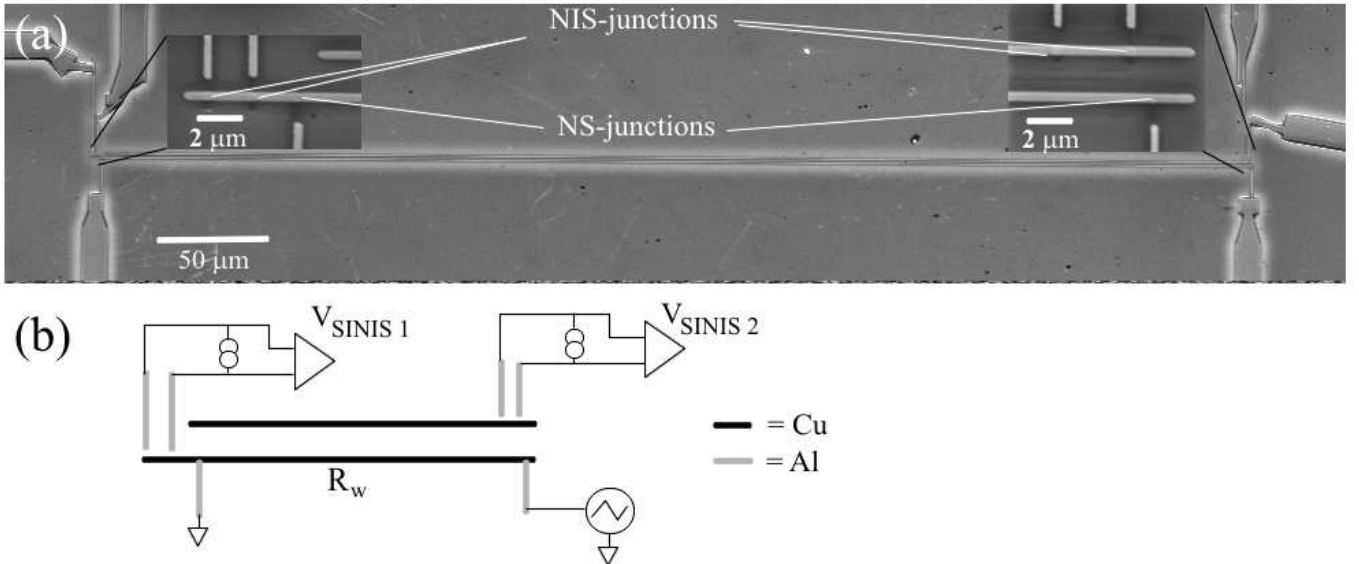


FIG. 1: (a) An SEM image of a sample. The horizontal lines are Cu wires, the vertical lines are Al leads that form the junctions at the intersections with the Cu line. The insets are enlargements of the areas where the junctions are located. Note that the pure Al vertical lines (black) make contact with the horizontal Cu lines, the lighter gray vertical lines consist of Al+shadows from the Cu evaporation. (b) A schematic of the sample and the measurement circuit.

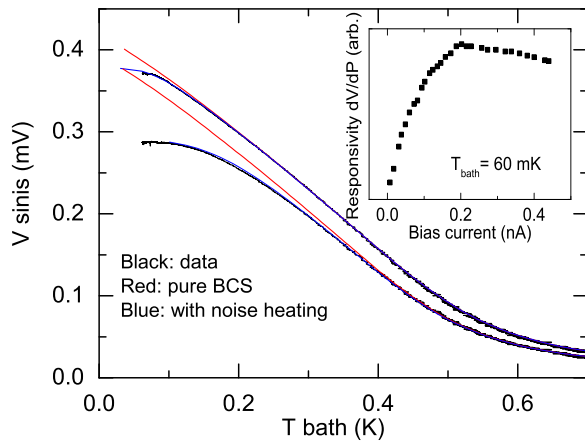


FIG. 2: (color) Calibration data for both SINIS tunnel junctions for the $t = 45 \text{ nm}$ sample, biased at $I = 200 \text{ pA}$. Black lines are the experimental data, red lines the BCS theory result, and blue lines the BCS-theory and a noise heating model, as explained in the text. The upper curves correspond to the wire with only a SINIS connected, the lower curves to the wire with both a SINIS and two NS-junctions. Δ and R_T were determined independently from the I-V characteristics. To obtain agreement with the calibration data Δ needed to be adjusted by $\sim 10 \%$ compared to the I-V value. From this data we estimate the temperature sensitivity $\delta T = (dT/dV)\delta V \approx 0.1 \text{ mK rms}$, where δV is the rms noise voltage. Inset: Measured responsivity dV/dP of a SINIS vs. the bias current.

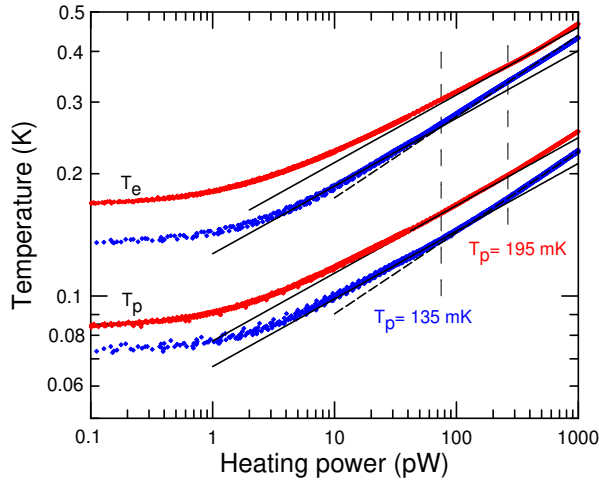


FIG. 3: (color) The electron (higher pair) and phonon (lower pair) temperatures of $t = 45$ nm (red) and $t = 90$ nm sample (blue) vs. applied Joule heating power in log-log scale. Straight lines are guides to the eye of the form $T = (P/A)^{1/6}$, corresponding to the disordered e-p scattering theory [Eq. (1)]. Dashed lines have $T = (P/A)^{1/5}$. Vertical lines mark the values of P where $ql = 1$. $T_{bath} = 60$ mK.

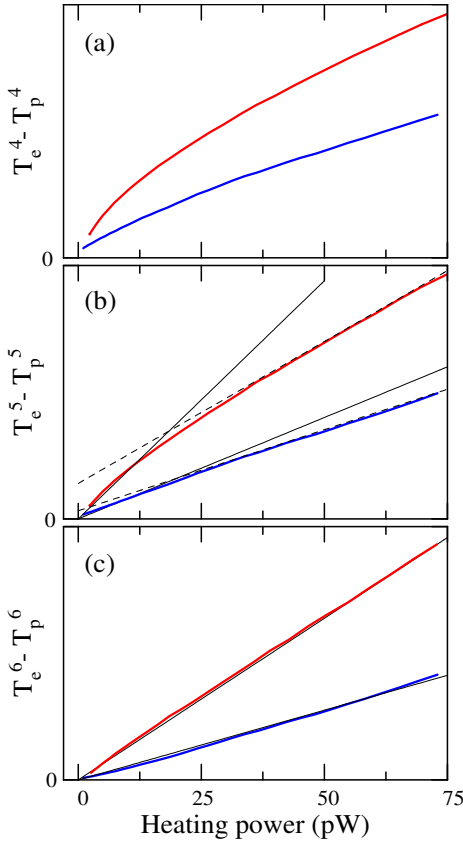


FIG. 4: (color) $T_e^n - T_p^n$ vs. Joule heating power (including a small noise power contribution ~ 1 pW, calculated from Fig. 3), with (a) $n = 4$, (b) $n = 5$, (c) $n = 6$. Red curves correspond to a thin sample ($t = 45$ nm), blue curves to a thick one ($t = 90$ nm). Straight lines are one parameter fits through the origin, dashed lines two parameter linear fits. $T_{bath} = 60$ mK.